Integrated Photonic Micro Logic Gate

Arkady Rudnitsky[1], Asaf Shahmoon[1], Menachem Nathan[2], Moshe Nazarathy[3], Bar Larom[3], Alexander Martucci[4], Luca Businaro[5], Annamaria Gerardino[6], and Zeev Zalevsky[1,*]

[1] School of engineering, Institute of Nanotechnology, Bar-Ilan University, Ramat-Gan, Israel
zalevsz@eng.biu.ac.il
[2] Faculty of Electrical Engineering, Tel-Aviv University, Israel
[3] Faculty of Electrical Engineering, Technion, Israel
[4] Università di Padova, Dipartimento Ingegneria Meccanica Set. Materiali, Padova, Italy
[5] LILIT Micro and nano fabrication Group, CNR-INFM TASC Laboratory, Trieste, Italy
[6] CNR – Inst. for photonics and nanotechnologies (IFM), Rome, Italy

Abstract. In this paper we present an approach for realizing an integrated all-optical logic gate. The basic principle is based upon stimulated emission process generated in an active gain medium while special interferometric photonic wave-guiding structure allows the realization of an integrated micro scale device. The operation rate of the proposed approach can theoretically reach tens of Tera-Hertz.

Keywords: All-optical devices; Photonic integrated circuits; Logic gates.

1 Introduction

Realizing optical integrated circuits is an important task due to both its scientific merit as well as its industrial applicability. The aim of this research is to generate all-optical integrated processing devices as modulators and logic gates capable of operating at high processing rates as well as being integrated with optics communication modules [1-6]. The ability to carry out concurrent large-scale on-chip information processing and multi-channel communication is valued in the information technology. All-optical systems may carry out these tasks at speeds or rates far exceeding electronic counterparts.

Typically, light beams which are to be processed by an all-optical device have a non-linearly interact with the electronic subsystem of the device's medium, so as to produce a certain non-linear effect (e.g. two and four waves mixing, frequency doubling, parametric oscillation, etc) on utilization of which the operation of the particular device is based. Accordingly, typical other approaches for realization of all-optical devices tend to use media with a large non-harmonicity of electronic oscillations. Typical all-optical devices also tend to require intense illumination and a large interaction length for proper operation [1-6].

* Corresponding author.

S. Dolev and M. Oltean (Eds.): OSC 2010, LNCS 6748, pp. 1–9, 2011.

In this paper we propose a new approach for an integrated all-optical logic gates capable of having nano and micro scale dimensions as well as ultra fast operation rates. The concept is based upon stimulated emission in pumped *gain medium* [7]. The technique utilizes the dependence of a signal propagating through a stimulated emission medium (herein called *gain medium*) on the gain. This dependence is typically non-linear with respect to the gain. The idea is that an input signals control the gain of the medium since the gain depends on the number of photons in the medium. Increasing the number of photons reduces the gain. Reference beam is passing through the gain medium and is coupled to the output of the device. Since the amplification of the medium is directly proportional to the logic inputs, a Boolean logic operation may be realized at the output of the device. Because a stimulated emission is involved the response rate of operation mechanism is very short (an immediate response).

The novelty of this paper includes also the design of special interferometric photonic wave-guiding structure which is a major component in the realization of an integrated micro scale logic device.

In section 2 we present the operation principle. Section 3 discuses the fabrication process of the device whose operation principle is being validated in section 4. The paper is concluded in section 5.

2 Operation Principle

The schematic sketch (see Fig. 1) for the basic all-optical logic gate contains a gain media which is pumped continuously from external source (not present in the Fig. 1). Reference beam is a continuously present beam. Output wave = Reference × G, where G is the gain factor of the gain media. There also two input signals to the logic gate. Those signals are used as the control signal for the gain media. If the control signal exists, the gain factor G is suppressed and the output beam exiting the gain module equals to zero. Only in the case when both of the control signals are zero (Input1 and Inout2 are both "0"), we have an amplified output beam coming from the output of the medium. This is a logical function "NOR". Although NOR is a universal Boolean operation in a sense that all other logic functions can be derived from it, the proposed concept can easily be used for realizing other logic functions as well. This to be further demonstrated in Section 4.

Mathematically the gain of a gain medium depends on the energy passing through it (in our case the pumping is always on) as follows:

$$\gamma = \frac{\gamma_0}{1 + \frac{I_v}{I_{sat}}} \tag{1}$$

where γ is the gain per unit length (overall gain G equals to $\exp(\gamma L)$ where L is the length of the gain medium), I_v is the energy in the gain medium and I_{sat} is the saturation energy level. From this equation it is simple to see that increasing the energy in the gain medium I_v, correspondingly reduces the overall gain.

The operation rate of the all-optical gate is very fast since, as seen in the rate equations for the amplification medium, the stimulated emission is a very fast

processes and basically depend only on the pumping power and the intensity developed in the medium (as presented in Eqs. 2 and 3) and not only on the spontaneous relaxation times:

$$\frac{dN_2}{dt} = R_p - \frac{N_2}{\tau_2} - (N_2 - N_1)W(\nu) \tag{2}$$

where N_2 and N_1 are the populations of the two levels between which the amplification is generated, R_p is the rate of pumping to the upper energetic level, τ_2 is the relaxation time related to the spontaneous processes, and W is related to the stimulated emission process and which is proportional to the intensity that is developed inside the medium:

$$W(\nu) = \frac{\kappa}{\nu^3} G(\nu) I_\nu \tag{3}$$

where κ is a constant, ν is the frequency, G is the gain spectral response and I_ν is the intensity in the gain medium.

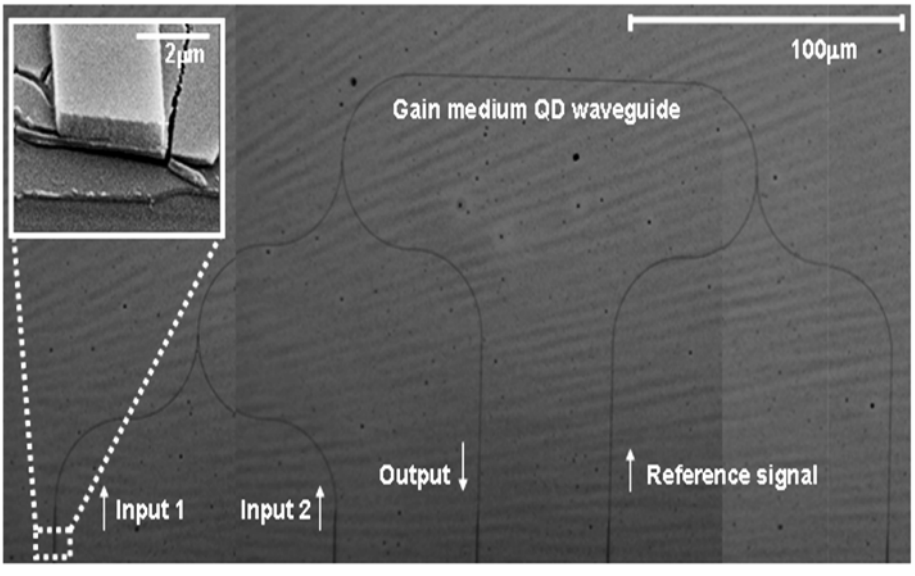

Fig. 1. Microscope image of the fabricated nano photonic device. On the upper left corner one may see the SEM image of the fabricated QD waveguide. The gain media is pumped continuously from external source which is not present in the figure.

3 Fabrication

The realization of an integrated all-optical circuit based upon gain medium can be obtained for instance by constructing optical waveguides in quantum dots (QD) photoresist [8,9]. The gain material is constantly pumped and thus following the rate equations of a gain medium, input signals passing through the medium at wavelength

corresponding to the gain/absorption spectral characteristics, will evoke immediate stimulated emission.

The microscope image of fabricated photonic chip following the above specified description may be seen in Fig. 1 (SEM image of the edge of the waveguide is seen in the upper left corner). The waveguide is made out of QD where on the left side we have the two logic inputs and on the right we input the reference beam. This reference is coupled to the right side of the chip where the output detector is located. The inputs affect the gain of the gain medium which controls the level of the reference beam that is going to the output. This yields, as previously explained, optical logic NOR gate.

The integrated chip option for realizing the proposed approach may include realization of the gain medium by fabricating ZrO_2 film (that was used as photo-resist) doped with CdSe@ZnS QDs which have a significant gain factor [8,9] over small interaction length. This fabrication process was applied to generate the chip seen in Fig. 1.

The X-ray diffraction (XRD) spectra of QD doped zirconia thin films at different annealing temperatures are seen in Fig. 2(a). A clear transition from amorphous to partially crystalline is observed above 400°C. Due to the low fill-factor of QDs in the sample (< 1% by volume) an effective medium model was not needed to account for the effect of the QD dispersion. Due to condensation of the matrix, a significant increase in the refractive index of the film and a concordant decrease in thickness were consistently observed with increasing annealing temperature. For example, following heat treatment at only 100°C, the average film refractive index n_g and thickness d (thin film of ZrO_2) were found to be 1.60 and 81nm respectively, while after annealing at 300°C these values changed to 1.75 (39 nm).

In addition to the usage of ZrO_2 thin films as the optical waveguide, there were attempts to fabricate waveguides out of TiO_2 film doped with CdSe@ZnS QD. For TiO_2 films following heat treatment at only 100 °C, the average film refractive index n_g and thickness d were found to be 1.69 and 54 nm respectively, while after annealing at 300 °C these values changed to 1.94 (31 nm). We found that in general n_g of TiO_2 films was 0.15 higher than values for ZrO_2 films at each studied annealing temperature. The XRD spectra of QD doped TiO_2 thin films at different annealing temperatures are seen in Fig. 2(b).

In Tables 1 and 2 one may find the summary of relevant parameters obtained for ZrO_2 and TiO_2 doped thin films respectively. In Tables 1and 2 n_d is the fully densified refractive index (anatase TiO_2 = 2.52, tetragonal ZrO_2 = 2.208) and n_g is the measured refractive index at the reference wavelength. The results in Tables 1 and 2 reveal that the overall film porosity significantly decreased for both matrices at higher annealing temperatures. This is expected due to the structural changes which occur during heating (i.e. removal of residual solvent and organics, to hydroxyl condensation and structural relaxation). The extent of densification of the ZrO_2 matrix was found to be very similar to that of the TiO_2 matrix at each studied annealing temperature. This similarity in densification rate led to the ZrO_2 matrix retaining a relatively high n_g value in comparison to TiO_2 at all the treatment temperatures.

From the fitted refractive index profiles and the film thickness, an estimation of the porosity for each sample was calculated using the Bruggeman model:

$$Porosity\,(\%) = \left(\left(\frac{n_d^{\,2} - n_g^{\,2}}{n_d^{\,2} + 2n_g^{\,2}} \right) \Big/ \left(\frac{n_d^{\,2} - n_g^{\,2}}{n_d^{\,2} + 2n_g^{\,2}} - \frac{1 - n_g^{\,2}}{1 + 2n_g^{\,2}} \right) \right) 100\% \tag{4}$$

Table 1. Summary of relevant parameters obtained for the ZrO_2 doped thin films

Matrix	n_e	Film Thickness (nm)	Porosity (%)	Min d/λ_0 Value for Guiding
ZrO_2-QD-100	1.601	81	47.53	0.234
ZrO_2-QD-200	1.683	56	41.35	0.165
ZrO_2-QD-300	1.753	39	36.05	0.132
ZrO_2-QD-400	1.794	30	32.93	0.118
ZrO_2-QD-500	1.829	27	30.26	0.108

Table 2. Summary of relevant parameters obtained for the TiO_2 doped thin films

Matrix	n_e	Film Thickness (nm)	Porosity (%)	Min d/λ_0 Value for Guiding
TiO_2-QD-100	1.693	54	50.99	0.160
TiO_2-QD-200	1.849	37	41.87	0.103
TiO_2-QD-300	1.935	31	36.81	0.085
TiO_2-QD-400	1.963	27	35.15	0.081
TiO_2-QD-500	2.006	24	32.59	0.074

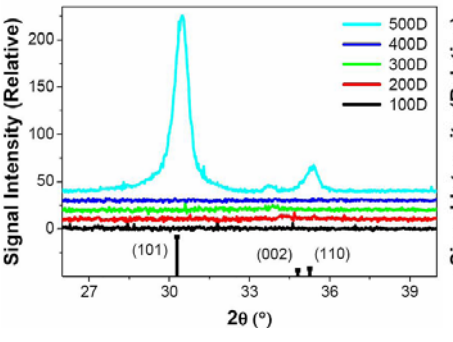

(a).

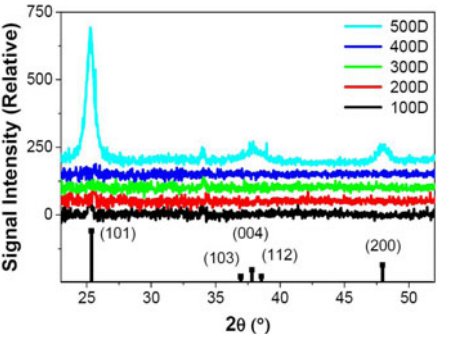

(b).

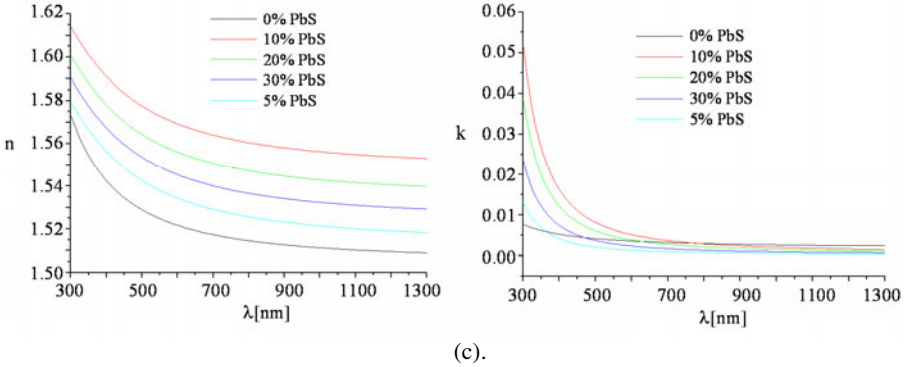

(c).

Fig. 2. (a). and (b). XRD spectra of ZrO_2 and TiO_2 films doped with CdSe@ZnS QDs annealed at 100, 200, 300, 400 and 500 °C, respectively. (c). Ellipsometry (real part n and imaginary part k of the refraction index) measurements on ZrO_2 film doped with PbS QDs annealed at 130 °C and containing 0, 5, 10, 20 and 30% of PbS.

In another fabrication attempt we used ZrO_2 film doped with PbS rather than CdSe@ZnS QD. The ellipsometry measurements (the real n and the imaginary k parts of the refraction index) on ZrO_2 film doped with PbS QD annealed at 130 °C and containing 0, 5, 10, 20 and 30% of PbS may be seen in Fig. 2(c). The introduction of lead sulphide increases both n (the real part of the refraction index) and k (the imaginary part of the refraction index).

4 Experimental Testing

Although we have fabricated the chip (Fig. 1), for the preliminary results of the experimental investigation we used the optical semiconductor amplifiers (SOA) [10,11] as the gain medium while the input signals are input through optical fibers. The bits of one of the input channels are delayed in comparison to the other. The purpose of the delay is to generate relative shift of half the pulse in order to demonstrate that even if the pulses are super imposed one on top of the other and the overall amplitude is increased, the output of the proposed device remains the same (due to the saturation of the gain medium). This is one of the very important advantages gained by the proposed approach. In the experimental investigation the modulation rate was 15MHz and the pulses width was 15nsec. As previously mentioned the SOA gain medium was constantly pumped.

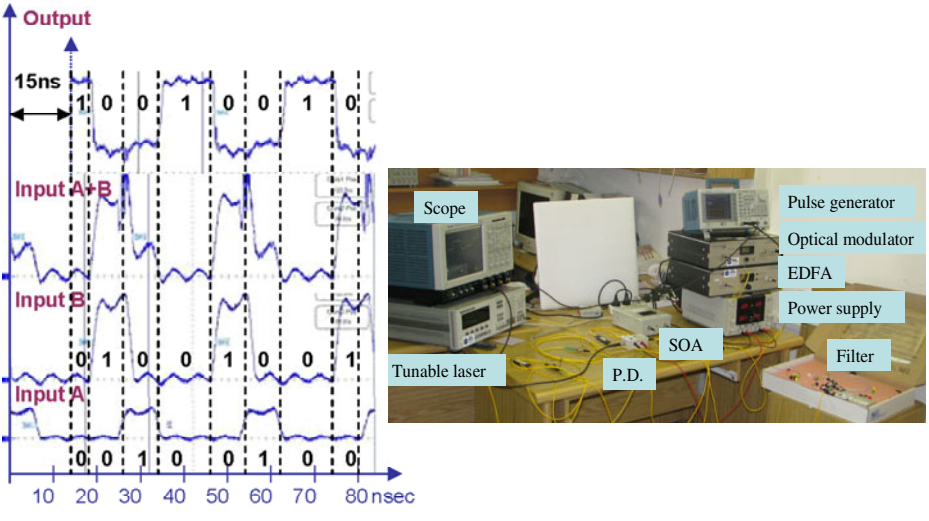

Fig. 3. Experimentally obtained preliminary results for all-optical logic NOR gate (using SOA). In the right part of the figure one may see image of the experimental setup as constructed in our laboratory.

In Fig. 3 one may see the measurements of input A, input B, both inputs together and the obtained output for that case respectively (going from the lower signals sequences presented in Fig. 3, upwards). From the results seen in Fig. 3 one may

conclude that only when both inputs A and B are zero the output is "1" otherwise it is "0". This is exactly the realization of the logic NOR gate operation. Note that the output channel as it is presented in Fig. 3 and which was captured by our scope was deliberately shifted in the time axis a shift of about 15nsec. We did this shift in the time axis in order to correct (or compensate) the temporal delay of about 15nsec (marked in the figure) that was generated due to the difference between the lengths of the cable that we used when connecting the input signals and the cable connecting the output of our device, to the scope channels.

In the right part of Fig. 3 we present the experimental setup that we used to produce the experimental results shown in the left part of the figure. The various electronic and optical components of the constructed measurements setup are indicated in the figure with proper labels.

Note that the proposed approach can be used for realizing different types of logic gates and not only the Boolean function of NOR. Figure 4(a) relates to the realization of a logic AND gate. The general structure for any logic function contains two parts: an integrated waveguide based interferometer and a gain medium. The output of the interferometer is input to the gain medium. In order to modify the Boolean function all that is required it to change the interferometer part while the gain medium module will remain unchanged. Thus, the difference between the AND gate in comparison to the previously discussed NOR gate is only in the interferometer part.

The interferometer part in the case of an AND gate includes three inputs: the two logic inputs (I_{in1} and I_{in2}) and a reference (I_{REF2}). The output of the interferometer is input to the gain medium. Another reference beam (I_{REF1}) is input to the gain medium and passed to the overall output of the logic gate (I_{out2}). The output of the

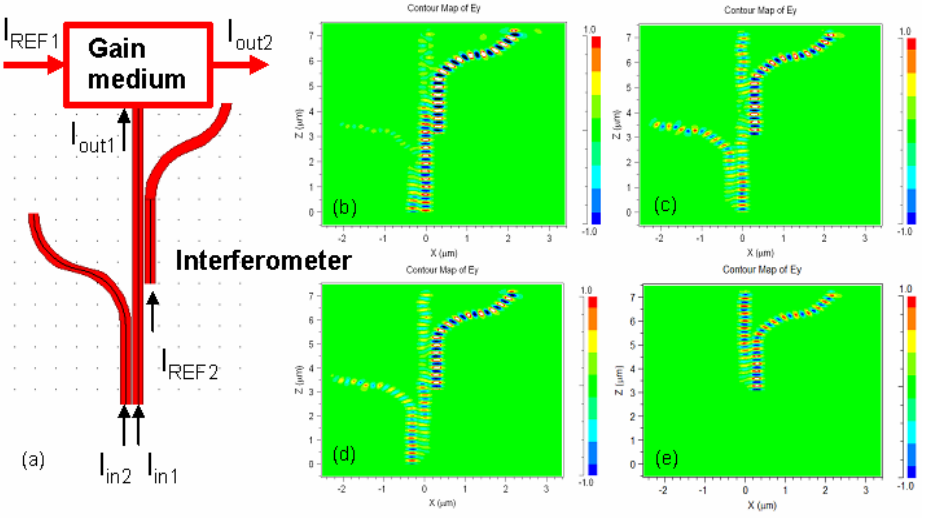

Fig. 4. (a). Schematic sketch of an AND logic gate. The interferometer which is later on simulated has inputs in its lower part and one output in its upper part. The right input is a reference. (b)-(e). Simulations of a nano metric interferometer. (b). I_{in1}= I_{in2}="1"; I_{out1}="0". (c). I_{in1}="1", I_{in2}="0"; I_{out1}="1". (d). I_{in1}="0", I_{in2}="1"; I_{out1}="1". (e). I_{in1}= I_{in2}="0"; Iout1="1".

Interferometer (I_{out1}) injects photons to the gain medium and therefore controls the gain level of the medium i.e. the gain applied over I_{REF1}. This results in obtaining the desired output from the device for proper combinations of the two logic inputs to the gate.

In Fig. 4(b)-4(e) we present the simulations of the interferometer device. All simulations presented in this section were done using numerical software of R-Soft using a Finite Difference Time Domain (FDTD) numerical approach in order to solve Maxwell's equations.

As seen from the simulations, the interferometer is designed such that its output equals to I_{REF2}- I_{in1}- I_{in2} (which is needed to obtain the overall AND functionality) while the energy of I_{REF2} is twice the energy of the two inputs such that only when both of them are present the output of the interferometer becomes zero (this by itself is similar to NAND functionality but when this logic combination illuminates the gain medium due to the fact that gain is reduced when the intensity of relevant photons is increased, the output of the overall device, i.e. the output of the gain medium, is logic one, i.e. a functionality of logic AND gate).

5 Conclusions

In this paper we have presented new concept of realizing ultra fast all-optical logic gates based upon the integration of a gain medium inducing stimulated emission and by that realizing the logic gate operation. Preliminary experimental results based upon SOA device as well as preliminary fabrication attempts of an integrated chip based upon of ZrO_2 and TiO_2 waveguides doped with quantum dots and their optical characterization were demonstrated.

References

1. Yabu, T., Geshiro, M., Kitamura, T., Nishida, K., Sawa, S.: All-optical logic gates containing a two-mode nonlinear waveguide. IEEE J. Quantu, Electron. 38, 37–46 (2002)
2. Yanik, M.F., Fan, S., Soljacic, M., Joannopoulos, J.D.: All-optical transistor action with bistable switching in a photonic crystal cross-waveguide geometry. Opt. Lett. 28, 2506–2508 (2003)
3. Buhl, L.L., Alferness, R.C.: Ti:LiNbO3 waveguide electro-optic beam combiner. Opt. Lett. 12, 778–780 (1987)
4. Lee, S.Y., Darmawan, S., Lee, C.W., Chin, M.K.: Transformation between directional couplers and multi-mode interferometers based on ridge waveguides. Opt. Exp. 12, 3079–3084 (2004)
5. Nagai, S., Morishima, G., Inayoshi, H., Utaka, K.: Multimode interference photonic switches. IEEE J. Lightwave Technol. 20, 675–681 (2002)
6. Zalevsky, Z., Rudnitsky, A., Nathan, M.: All-optical devices and methods for data processing. Patent application # 166810 (2005)
7. Zalevsky, Z., Rudnitsky, A.: Devices and methods for optical signal control. Patent application #12/401 779 (2007)

8. Jasieniak, J.J., Fortunati, I., Gardin, S., Signorini, R., Bozio, R., Martucci, A., Mulvaney, P.: Highly efficient amplified stimulated emission from CdSe-CdS-ZnS quantum dot doped waveguides with two-photon infrared optical pumping. Adv. Mater. 20, 69–73 (2007)
9. Jasieniak, J.J., Pacifico, J., Signorini, R., Chiasera, A., Ferrari, M., Martucci, A., Mulvaney, P.: Luminescence and amplified stimulated emission in CdSe-ZnS-nanocrystal-doped TiO2 and ZrO2 waveguides. Adv. Funct. Mater. 17, 1654–1662 (2007)
10. Kim, Y., Kim, J.H., Jeon, Y.M., Lee, S., Woo, D.H., Kim, S.H., Yoon, T.: All-optical flip-flop based on optical bistability in an integrated SOA/DFB-SOA. In: Sawchuk, A. (ed.) Optical Fiber Communications Conference. OSA Trends in Optics and Photonics (Optical Society of America, 2002), vol. 70 (2002) paper TuF5
11. Ono, H., Yamada, M., Shimizu, M.: S-Band EDFA with multistage configuration design, characterizations and gain tilt compensation. J. of Lightwave Tech. 21, 2240–2247 (2003)